

contribute to HRV-specific IRES translation mechanisms, ORF termination, or polymerase recognition. We also found embedded within multiple sequences, including recent field isolates, clear evidence for repeated, historical genome recombination. Coinfection with multiple HRVs is known to occur (28), and we now know that this can lead to strains that may have distinct biologic properties and clinical characteristics. The required host environment for HRV recombination is not known, but with complete genome sequences from additional patient isolates such factors may become apparent. Our repository data set provides a baseline framework for the analysis of additional HRVs that may be in communities, including the HRV-Cs, and will enable larger-scale studies of basic molecular and evolutionary characteristics and assignment of disease phenotypes to specific genome regions. The clustering of small clades, the recombinations, and the mutations found in all regions of these genomes suggest that future HRV epidemiologic studies might benefit from full genome sequencing rather than the more limited serotyping. With such an approach, correlations may be more informative in inferring pathogenic potential and in designing antiviral agents and vaccines.

References and Notes

1. J. M. Gwaltney Jr., J. O. Hendley, G. Simon, W. S. Jordan Jr., *N. Engl. J. Med.* **275**, 1261 (1966).
2. S. L. Johnston *et al.*, *Am. J. Respir. Crit. Care Med.* **154**, 654 (1996).
3. K. G. Nicholson, J. Kent, D. C. Ireland, *Br. Med. J.* **307**, 982 (1993).
4. D. J. Jackson *et al.*, *Am. J. Respir. Crit. Care Med.* **178**, 667 (2008).
5. A. M. Fendrick, A. S. Monto, B. Nightengale, M. Sarnes, *Arch. Intern. Med.* **163**, 487 (2003).
6. K. B. Weiss, S. D. Sullivan, *J. Allergy Clin. Immunol.* **107**, 3 (2001).
7. M. Vlasak *et al.*, *J. Virol.* **79**, 7389 (2005).
8. K. Andries *et al.*, *J. Virol.* **64**, 1117 (1990).
9. S. R. Dominguez *et al.*, *J. Clin. Virol.* **43**, 219 (2008).
10. P. McErlean *et al.*, *PLoS ONE* **3**, e1847 (2008).
11. S. K. Lau *et al.*, *J. Clin. Microbiol.* **45**, 3655 (2007).
12. A. Djikeng *et al.*, *BMC Genomics* **9**, 5 (2008).
13. Materials and methods are available as supporting material on Science Online.
14. A. C. Palmenberg, J.-Y. Sgro, in *Molecular Biology of Picornaviruses*, B. L. Semler, E. Wimmer, Eds. (ASM Press, New York, 2001).
15. A. C. Palmenberg, J.-Y. Sgro, *Semin. Virol.* **8**, 231 (1997).
16. L. R. Martin, G. M. Duke, J. E. Osorio, D. J. Hall, A. C. Palmenberg, *J. Virol.* **70**, 2027 (1996).
17. R. J. Jackson, in *Translational Control*, W. B. Hershey, M. B. Mathews, N. Sonenberg, Eds. (Cold Spring Harbor Laboratory Press, Cold Spring Harbor, NY, 1996).
18. K. Tamura, J. Dudley, M. Nei, S. Kumar, *Mol. Biol. Evol.* **24**, 1596 (2007).
19. On the basis of these data, the International Committee on Taxonomy of Viruses Picornavirus Study Group recently proposed to recognize them as a new species (29).
20. hrv-08 and hrv-95 are designated as two different serotypes by ATCC but differ by 67 nucleotides, perhaps indicating a misidentification in the repository.
21. R. M. Ledford *et al.*, *J. Virol.* **78**, 3663 (2004).
22. C. Savolainen, S. Blomqvist, M. N. Mulders, T. Hovi, *J. Gen. Virol.* **83**, 333 (2002).
23. A. L. Kistler *et al.*, *Virology* **4**, 40 (2007).
24. P. Simmonds, *J. Virol.* **80**, 11124 (2006).
25. D. Martin, E. Rybicki, *Bioinformatics* **16**, 562 (2000).
26. R. Fleischer, K. Laessig, *Clin. Infect. Dis.* **37**, 1722 (2003).
27. D. L. Barnard, *Curr. Pharm. Des.* **12**, 1379 (2006).
28. C. Savolainen, M. N. Mulders, T. Hovi, *Virus Res.* **85**, 41 (2002).
29. N. Knowles, personal communication.
30. Funded by the University of Maryland School of Medicine internal funds and by NIH grant U19-AI070503. We thank A. Wolf and J.-Y. Sgro for implementation of the tree topology tests. The accession numbers for the hrv strains are FJ445111 to FJ445190 (see table S1).

Supporting Online Material

www.sciencemag.org/cgi/content/full/1165557/DC1

Materials and Methods

Figs. S1 to S6

Tables S1 to S5

References

5 September 2008; accepted 4 February 2009

Published online 12 February 2009;

10.1126/science.1165557

Include this information when citing this paper.

REPORTS

Photodegradable Hydrogels for Dynamic Tuning of Physical and Chemical Properties

April M. Kloxin,¹ Andrea M. Kasko,^{1,2*} Chelsea N. Salinas,¹ Kristi S. Anseth^{1,2,†}

We report a strategy to create photodegradable poly(ethylene glycol)-based hydrogels through rapid polymerization of cytocompatible macromers for remote manipulation of gel properties *in situ*. Postgelation control of the gel properties was demonstrated to introduce temporal changes, creation of arbitrarily shaped features, and on-demand pendant functionality release. Channels photodegraded within a hydrogel containing encapsulated cells allow cell migration. Temporal variation of the biochemical gel composition was used to influence chondrogenic differentiation of encapsulated stem cells. Photodegradable gels that allow real-time manipulation of material properties or chemistry provide dynamic environments with the scope to answer fundamental questions about material regulation of live cell function and may affect an array of applications from design of drug delivery vehicles to tissue engineering systems.

Hydrogels are hydrophilic polymers swollen by water that are insoluble owing to physical or chemical cross-links. These water-swollen gels are used extensively as biomaterials for complex device fabrication (1), cell culture for

tissue regeneration (2), and targeted drug release (3). Often, sophisticated control of the gel structure in space and time is required to elucidate the dynamic relationship between biomaterial properties and their influence on biological function (4, 5). For example, progenitor cells are often expanded and differentiated in hydrogel microenvironments, and researchers have demonstrated how the initial gel properties, including mechanics (6, 7) and chemical functionality (8), influence cellular fate. In regenerative medicine, the structure and composition of gels are also regulated temporally, through hydrolytic (9) and enzymatic (10–12) degradation mech-

anisms, to promote cell secretory properties and encourage the development of tissue-like structures *in vitro* and *in vivo*. A major challenge is determining which biochemical and biophysical features must be presented in a gel culture environment.

Hydrogel structure and functionality have evolved from the direct encapsulation of cells in simple homogeneous materials to those with highly regulated structures spanning multiple size scales [e.g., through self-assembly (13) or micro-engineering (14)]. These hydrogel structures are further modified locally by cells with the synthetic incorporation of bioresponsive functionalities (15) or externally by advanced patterning to create spatially varying functionalities. For example, the chemical patterning of a gel by the addition of a second, interpenetrating network or peptide tether has been demonstrated by diffusing chemical moieties into a gel and covalently linking these functionalities to the network by photocoupling (16) or reaction with a photolytically uncaged reactive group (17). Although these are important advances, such processes do not allow modulation of the gel chemistry in real time or photodegradation of the gel structure. Few synthetic materials provide a cellular microenvironment in which physical or chemical cues are initially present and subsequently regulated on demand. We have synthesized monomers capable of polymerizing in the presence of cells to produce photolytically degradable hydrogels whose physical or chemical properties are tunable temporally and spatially with light. The desired gel property for altering cell function or fabricating a

¹Department of Chemical and Biological Engineering, University of Colorado, 424 UCB ECCH 111, Boulder, CO 80309, USA. ²Howard Hughes Medical Institute, University of Colorado, 424 UCB ECCH 111, Boulder, CO 80309, USA.

*Present address: Department of Bioengineering, University of California, Los Angeles, CA, 90095–1600, USA.

†To whom correspondence should be addressed. E-mail: Kristi.Anseth@colorado.edu

device is thus externally triggered and directed with irradiation by photolytic cleavage and removal of the macromolecules that compose the gel.

The photodegradable functionality, a nitrobenzyl ether-derived moiety, was selected based on its photolytic efficiency, susceptibility to two-photon photolysis, and previous use in live cell culture and imaging (18, 19). Similar photolabile functionalities have been used in multistep gel-modification processes (20). A base photodegradable monomer was synthesized by acrylation of the photolabile moiety by a pendant hydroxyl group [photodegradable acrylate (PDA)] (Fig. 1A) and was subsequently attached with a pendant carboxylic acid to poly(ethylene glycol) (PEG)-*bis*-amine to create a photocleavable cross-linking diacrylate macromer (Compound 1, Fig. 1B) from which PEG-based photodegradable hydrogels (Fig. 1C) were synthesized. This approach, in which the photolabile moiety is incorporated within the network backbone, is fundamentally different from strategies in which reactive groups or biomolecules are asymmetrically caged or capped by a photolabile group (20). Here, the hydrogel itself is cleaved upon light exposure, decreasing the local network cross-link density and resulting in macroscopic property changes such as stiffness, water content, diffusivity, or complete erosion, all in the presence of cells.

The photodegradable cross-linker, Compound 1, was copolymerized with PEG monoacrylate (PEGA) in phosphate-buffered saline (PBS) by redox-initiated free radical polymerization to create photodegradable hydrogels. Upon irradiation, these hydrogels release modified PEG, and after complete degradation they release modified poly(acrylate) chains, as shown in Fig. 1C. The bulk photodegradation of these hydrogels, ensured by flood irradiation through a small thickness of material, was characterized within a parallel-plate rheometer (21). The storage modulus (G') is proportional to the hydrogel cross-linking density (ρ_x) (22, 23), allowing calculation of the characteristic photolabile group degradation time (τ) when normalized to its initial value (G'_0) via $G'/G'_0 = \rho_x/\rho_{x0} = \exp(-2t/\tau)$. At an irradiation intensity of 10 mW/cm² at 365 nm, typical irradiation conditions for hydrogel photopolymerizations in the presence of cells (24), the hydrogel completely degrades in 10 min ($\tau \sim 280$ s) (Fig. 1D). As expected from photolysis kinetics (supporting online text), doubling the intensity halves the time to complete degradation ($\tau \sim 140$ s) (Fig. 1D), whereas irradiation at 405 nm increases the degradation time inversely with the relative molar absorptivity ($\tau \sim 930$ s) (Fig. 1D). When the irradiation is ceased, the degradation is arrested; degradation is recommenced upon further irradiation (Fig. 1E). The degradation rate and extent and the resulting material properties such as stiffness thus can be predictably manipulated with light intensity and wavelength.

Precise control of gel cross-linking density was used to examine the influence of gel structure on cell spreading. Specifically, human mesenchymal stem cells (hMSCs) were encapsulated within a densely cross-linked gel where they exhibit a

rounded morphology (Fig. 1F). When the gel cross-linking density was reduced through photodegradation, cell spreading was observed (Fig. 1G), whereas the cell viability was maintained (fig. S4). Thus, cell morphology can be manipulated by irradiation and degradation of these hydrogels at any time in culture. Although this control can be useful for allowing cell spreading or extracellular matrix (ECM) elaboration, this molecular-scale degradation does not allow for bulk cell migration or long-range cell-cell interactions, which require fabrication of micron-scale channels by gel erosion.

To study gel erosion, degradation was first confined to the irradiation surface by selecting an irradiation wavelength that corresponds to a high photolabile group molar absorptivity (fig. S1). Because the light intensity is highest within the

uppermost layers of a thick gel, these top layers erode away rapidly during light exposure before degradation of underlying layers (see schematic, Fig. 2A). Irradiation of a hydrogel through a photomask degrades the material in the exposed regions and creates progressively recessed areas, whereas material in the unexposed areas remains intact (see photographic series, Fig. 2A). Profilometry reveals well-defined ridges, demonstrating reproduction of the irradiation pattern, and feature height increases linearly with exposure time (Fig. 2A). Such photolithographic techniques at highly absorbed wavelengths can be used to create surface features of varying height and width postgelation, while avoiding concomitant dimension changes in the hydrogel bulk, useful for the fabrication and subsequent manipulation of cell culture devices.

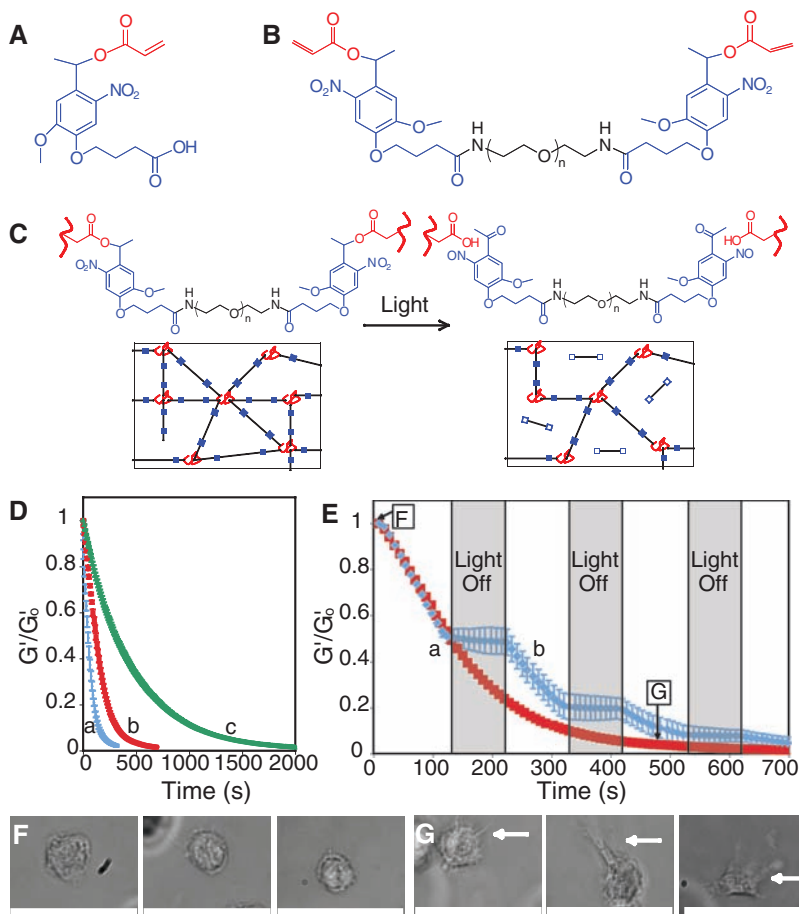


Fig. 1. Photodegradable hydrogel synthesis and degradation for tuning gel properties. **(A)** The base photodegradable acrylic monomer was used to synthesize **(B)** the photodegradable cross-linking macromer (Compound 1, $M_n \sim 4070$ g/mol), composed of PEG (black), photolabile moieties (blue), and acrylic end groups (red). **(C)** Compound 1 was copolymerized with PEGA ($M_n \sim 375$ g/mol), creating gels composed of poly(acrylate) chains (red coils) connected by PEG (black lines) with photolabile groups (solid blue boxes) (left). Upon irradiation, the photolabile moiety cleaves (open blue boxes), decreasing ρ_x and releasing modified PEG (right). **(D)** The physical structure of the hydrogel is degraded by photolysis, decreasing ρ_x and G' . The influence of irradiation on G' , normalized to G'_0 , was monitored with rheometry. The degradation rate was precisely controlled with irradiation intensity and wavelength: (a) 365 nm at 20 mW/cm², (b) 365 nm at 10 mW/cm², and (c) 405 nm at 25 mW/cm². **(E)** The gel degradation was modulated by either (a) continuous or (b) periodic irradiation with 365 nm at 10 mW/cm². The extents of degradation corresponding to the materials used in Fig. 1, F and G, are indicated. **(F)** hMSCs encapsulated within dense hydrogels exhibit a rounded morphology. **(G)** Irradiation (480 s, 365 nm at 10 mW/cm²) significantly degrades the gel ($\rho_x/\rho_{x0} \sim 0.04$), promoting hMSC spreading after 3 days in culture. Scale bar, 50 μ m.

Controlled creation of three-dimensional (3D) cell culture microenvironments facilitates the examination of cell-matrix and cell-cell interactions. The postgelation addition of chemical moieties, such as peptides, to hydrogels in three dimensions has been demonstrated in a multistep technique using a two-photon laser scanning microscope (LSM) (16, 17). Using a photodegradable hydrogel in conjunction with a single (405 nm) (fig. S2) or two-photon (740 nm) LSM (Fig. 2B), we gen-

erated 3D features within a hydrogel by local photodegradation with scan parameters similar to those used for cell imaging and without the addition of chemical moieties. This rapid patterning (seconds to minutes) is achieved by controlled rastering of the laser focus within the hydrogel, locally degrading the polymer network and creating arbitrary 3D features on the micron scale (schematic, Fig. 2B). Interconnected channels, potentially useful for directing cell connectivity and/or migra-

tion, were created within a rhodamine-labeled photodegradable hydrogel with a two-photon LSM and visualized using brightfield and fluorescence microscopy (Fig. 2B). Other features of arbitrary shape and size for desired applications such as device fabrication can be precisely and rapidly patterned within these photodegradable hydrogels in situ using either a single or two-photon LSM with standard imaging parameters (fig. S2).

To demonstrate how erosion of these photodegradable hydrogels can be used to direct cell migration, fibrosarcoma cells were encapsulated within a hydrogel. A portion of these entrapped cells was subsequently released by degrading channels within the gel using photolithography. Cells near the periphery of the channel were then allowed to migrate along the channel length (Fig. 2C). With the ability to pattern microscopic to macroscopic structures in the presence of encapsulated cells, these photodegradable hydrogels provide a cell culture platform to allow unique studies of directed cell migration (25, 26) and cell connectivity (27) by enabling real-time manipulation of the cell microenvironment. It is important to note, however, that cell migration exclusively occurs in regions of complete or near-complete gel erosion. In many cases, the culturing of cells in an environment that allows bulk migration is desirable, with subsequent direction of cell-cell interactions at a certain point in time or space. To achieve this, complementary chemistries, such as enzymatically degradable moieties, can be incorporated within these gels by, for example, Michael addition (9) of the photodegradable cross-linker with an enzymatically cleavable, thiol-containing peptide (2).

The aforementioned techniques have focused on the patterning of hydrogels for degradation of the physical network structure; however, photodegradable linkages can also be exploited to locally modify the chemical environment within a hydrogel by incorporation of tethered, but photolabile, biologically active functionalities. To demonstrate, the PDA monomer was coupled through its pendant carboxylic acid to the ubiquitous adhesion peptide sequence Arg-Gly-Asp-Ser (RGDS) (28), producing an asymmetric, photodegradable, bifunctional acrylic monomer (Fig. 3A). Copolymerization of this photoreleasable macromer with a nondegradable PEG diacrylate (PEGDA) yields a hydrogel with photolytic control over its chemical interaction with encapsulated cells (Fig. 3B). Upon irradiation, the modified peptide is cleaved from the polymer network and released into solution, where it quickly diffuses out of the gel (fig. S3). Peptide presentation within the microenvironment can thus be controlled with irradiation at a rate based on the photolabile group characteristic degradation time (Fig. 1D). More generally, this technique can be used for controlling the chemical structure of hydrogels in three dimensions and in time, where the peptide RGDS can be replaced with any biomolecule of interest, creating an additional tool for the modulation of ligand presentation (4).

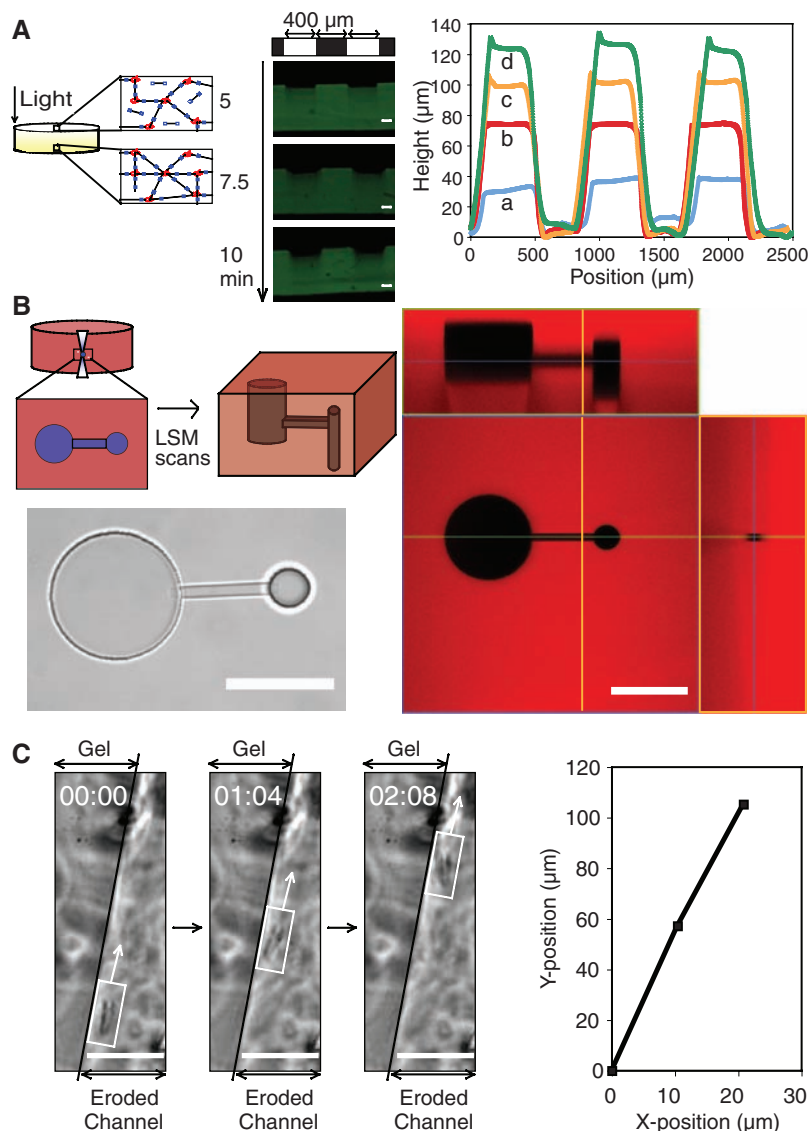


Fig. 2. 2D and 3D patterning of photodegradable hydrogels. **(A)** Thick gels demonstrate surface erosion upon irradiation (left). A gel covalently labeled with fluorescein was eroded spatially through masked flood irradiation (320 to 500 nm at 40 mW/cm², 400 μm line periodic photomask). Channel depth increased linearly with irradiation, and no changes in hydrogel dimensions due to increased swelling were observed (middle). Feature dimensions were quantified with profilometry: (a) 2.5, (b) 5, (c) 7.5, and (d) 10 min irradiation (right). Scale bar, 100 μm. **(B)** Interconnected 3D channels were fabricated within a photodegradable gel, covalently labeled with rhodamine B, using a two-photon LSM. A thin horizontal channel connected two offset vertical channels of different diameter, which was visualized in brightfield (bottom left) and with confocal LSM (right, intact gel is red and the created feature is black; corresponding cross sections are noted by blue, green, and orange lines). Scale bar, 100 μm. **(C)** Channels were eroded within a hydrogel encapsulating fibrosarcoma cells, releasing cells into the degraded channel and enabling migration. Migration of a cell along the edge of a channel is shown in time-lapsed brightfield images (left) and its corresponding position trace (right). Scale bar, 50 μm.

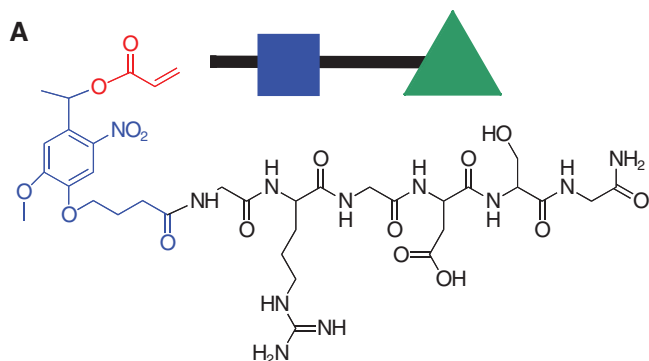


Fig. 3. Photolabile RGDS tether synthesis and use for dynamic changes in microenvironment chemistry. **(A)** A photolabile asymmetric biofunctional acrylic monomer (Compound 2) was synthesized containing the adhesion peptide RGDS (black) attached to the PDA (acrylate in red and photolabile moiety in blue). **(B)** Compound 2 was polymerized (green triangle with closed blue box) into a nondegradable gel (red poly(acrylate) coils connected by black nondegradable PEG cross-links) whose chemical composition is controlled with light exposure by photolytic release of the tethered biomolecule RGDS (bottom, green triangle with open blue box). hMSCs were encapsulated in nondegradable PEG gels (b) with or (a) without photoreleasable RGDS. The presentation of RGDS was temporally altered by (c) photocleavage of RGDS from the gel on day 10 in culture. **(C)** RGDS presentation maintains hMSC viability within PEG-based gels (inset table). RGDS photolytic removal on day 10 directs hMSC chondrogenesis, (c) increasing GAG production four-fold over (b) persistently presented RGDS or (a) PEG-only gels by day 21 ($P < 0.05$), an indicator of hMSC chondrogenesis.

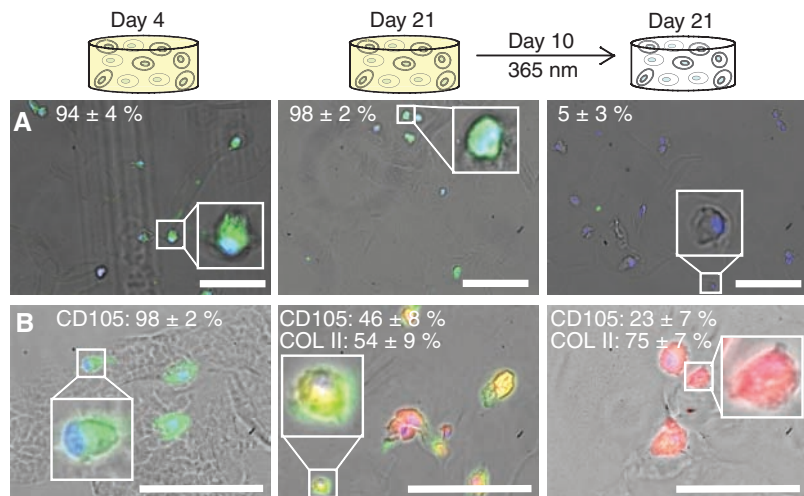
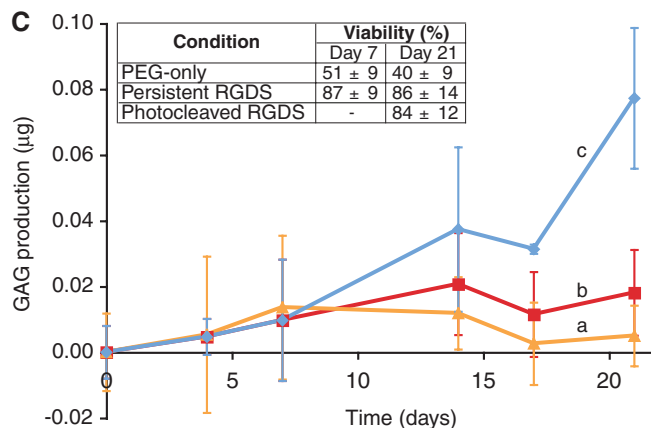
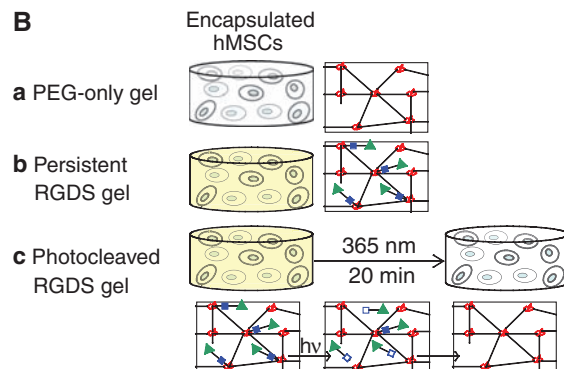


Fig. 4. Influence of dynamic microenvironment chemistry on integrin expression and differentiation. **(A)** Cells (4',6'-diamidino-2-phenylindole-labeled nuclei, blue) cultured with persistent RGDS express the cell-surface integrin $\alpha_v\beta_3$ (fluorescein isothiocyanate-labeled, green) on day 4 (left) and day 21 (middle) in culture. Cells with photocleaved RGDS have decreased expression of the $\alpha_v\beta_3$ integrin by day 21 (right), indicating that the cells have responded to the removal of RGDS. (Representative images shown with average cell percentages noted.) **(B)** Chondrogenic differentiation of hMSCs was verified by immunostaining for the hMSC marker CD105 (FITC, green) and the chondrocyte marker COLII (tetramethyl rhodamine isothiocyanate-labeled, red). Within error, no cells initially produce COLII (day 4, left). By day 21, half of the cells presented persistently with RGDS strongly expressed CD105, and the other half produced COLII (middle). With photolytic removal of RGDS on day 10, one-fourth of the cells strongly expressed CD105 and three-fourths produced COLII (right), supporting that photolytic removal of RGDS increases chondrogenesis. (Representative images shown with average cell percentages strongly expressing the marker noted.) Scale bars, 100 μ m.

To demonstrate the utility of this photolabile tether platform, hMSCs were encapsulated in nondegradable PEGDA hydrogels, both with and

without the photoreleasable RGDS moiety, to examine the effect of temporal RGDS presentation on hMSC viability and chondrogenic dif-

ferentiation. Control of the local biochemical environment enables promotion of chondrogenesis. Although numerous researchers have incorporated the fibronectin epitope RGD into biomaterial microenvironments to promote the survival of hMSCs (5, 29, 30), few studies investigate the importance of the persistence of this signal on the differentiation fate (31–33). Natively, hMSCs differentiating into chondrocytes initially produce the adhesion protein fibronectin, which is subsequently down-regulated between days 7 and 10, while the excreted ECM is remodeled through enzyme production (31, 34). After day 10, these cells up-regulate production of glycosaminoglycans (GAGs) and type II collagen (COLII), two major components of cartilage and specific indicators of chondrogenic differentiation (31, 34). To examine this temporal change in vitro, a portion of the cell-gel constructs containing the photolabile RGDS tether were irradiated on day 10 in culture to remove the fibronectin epitope RGDS from the encapsulated cell microenvironment (Fig. 3B).

The absence of RGDS in 3D cell culture yields a statistically significant decrease ($P < 0.05$) in hMSC viability within the first 7 days in PEG-only gels (see inset, Fig. 3C), in agreement with other experimental results (29, 30) (supporting online text). Upon photolytic removal of RGDS from the photolabile tether gels on day 10, cell viability was unaffected; however, by day 21, a four-fold statistical increase ($P < 0.05$) in the production GAGs occurred relative to the persistently presented RGDS or PEG-only hydrogels, indicating further differentiation of the hMSCs

down the chondrogenic pathway in response to the microenvironment modification (Fig. 3C and fig. S5). To examine cell interaction with this dynamic microenvironment, fixed sections were immunostained for the expression of the $\alpha_v\beta_3$ integrin, one of the cell surface integrins by which cells interact with RGDS. Cells persistently presented with RGDS express the integrin, whereas most cells with RGDS photoreleased cease integrin expression by day 21 (Fig. 4A), indicating that the cells have locally sensed and responded to the chemical change in their environment. Additionally, to determine that the elevated GAG production is associated with chondrogenesis, sections of the cell-hydrogel constructs were immunostained for the hMSC marker CD105 (transforming growth factor- β receptor) and the chondrocyte marker COLII. As hMSCs differentiate into chondrocytes in 3D culture, a decrease in CD105 expression is observed along with onset of COLII production (35). The photolytic removal of RGDS on day 10 is accompanied by a decrease in CD105 expression and elevated COLII production as compared with persistently presented RGDS on day 21 (Fig. 4B), indicating increased chondrogenesis. With this photodegradable tether approach, the dynamic influence of other biomolecules on cell function can be similarly studied, expanding the ability to fabricate material environments that control cell function. Although manipulation of a single signal was examined and used to direct hMSC differentiation herein, this gel system can be readily functionalized with photolabile moieties of different light absorbances and cleavage efficiencies, enabling independent control over multiple signals through selection of irradiation wavelength and intensity.

We have demonstrated the synthesis of photodegradable macromers and their subsequent polymerization to form hydrogels whose physical, chemical, and biological properties can be tuned in situ and in the presence of cells by ultraviolet, visible, or two-photon irradiation. These photo-

degradable hydrogels show promise as in vitro 3D cell culture platforms in which cell-material interactions are dynamically and externally directed to elucidate how cells receive and process information from their environments. Ways to promote or suppress desired cell functions may become possible with temporal and spatial regulation of the 3D culture microenvironment, leading to applications in fields ranging from controlled drug delivery to tissue regeneration.

References and Notes

- D. B. Weibel, W. R. DiLuzio, G. M. Whitesides, *Nat. Rev. Microbiol.* **5**, 209 (2007).
- M. P. Lutolf, J. A. Hubbell, *Nat. Biotechnol.* **23**, 47 (2005).
- R. Langer, N. A. Peppas, *AIChE J.* **49**, 2990 (2003).
- M. M. Stevens, J. H. George, *Science* **310**, 1135 (2005).
- G. Chan, D. J. Mooney, *Trends Biotechnol.* **26**, 382 (2008).
- A. J. Engler, S. Sen, H. L. Sweeney, D. E. Discher, *Cell* **126**, 677 (2006).
- A. J. Engler et al., *J. Cell Biol.* **166**, 877 (2004).
- P. A. Kenny, M. J. Bissell, *Int. J. Cancer* **107**, 688 (2003).
- A. Metters, J. Hubbell, *Biomacromolecules* **6**, 290 (2005).
- M. A. Rice, J. Sanchez-Adams, K. S. Anseth, *Biomacromolecules* **7**, 1968 (2006).
- D. Seliktar, A. H. Zisch, M. P. Lutolf, J. L. Wrana, J. A. Hubbell, *J. Biomed. Mater. Res. Part A* **68A**, 704 (2004).
- M. Ehrbar et al., *Circ. Res.* **94**, 1124 (2004).
- G. A. Silva et al., *Science* **303**, 1352 (2004).
- A. Khademhosseini, R. Langer, *Biomaterials* **28**, 5087 (2007).
- R. W. Sands, D. J. Mooney, *Curr. Opin. Biotechnol.* **18**, 448 (2007).
- M. S. Hahn, J. S. Miller, J. L. West, *Adv. Mater.* **18**, 2679 (2006).
- J. H. Wosnick, M. S. Shoichet, *Chem. Mater.* **20**, 55 (2008).
- Y. R. Zhao et al., *J. Am. Chem. Soc.* **126**, 4653 (2004).
- M. Alvarez et al., *Adv. Mater.* **20**, 4563 (2008).
- Y. Luo, M. S. Shoichet, *Nat. Mater.* **3**, 249 (2004).
- S. A. Khan, I. M. Plitz, R. A. Frantz, *Rheol. Acta* **31**, 151 (1992).
- R. J. Young, P. A. Lovell, *Introduction to Polymers* (Chapman & Hall, London, ed. 2, 1991).
- S. J. Bryant, K. S. Anseth, in *Scaffolding in Tissue Engineering*, P. X. Ma, J. Elisseeff, Eds. (Marcel Dekker, New York, 2005), pp. 69–88.

- S. J. Bryant, C. R. Nuttelman, K. S. Anseth, *J. Biomater. Sci. Polym. Ed.* **11**, 439 (2000).
- P. Tayalia, C. R. Mendonca, T. Baldacchini, D. J. Mooney, E. Mazur, *Adv. Mater.* **20**, 4494 (2008).
- G. P. Raebler, M. P. Lutolf, J. A. Hubbell, *Biophys. J.* **89**, 1374 (2005).
- M. J. Mahoney, K. S. Anseth, *Biomaterials* **27**, 2265 (2006).
- E. Ruoslahti, M. D. Pierschbacher, *Science* **238**, 491 (1987).
- T. Boontheekul, D. J. Mooney, *Curr. Opin. Biotechnol.* **14**, 559 (2003).
- G. A. Hudalla, T. S. Eng, W. L. Murphy, *Biomacromolecules* **9**, 842 (2008).
- S. Tavella et al., *J. Cell Sci.* **110**, 2261 (1997).
- C. R. Nuttelman, M. C. Tripodi, K. S. Anseth, *Matrix Biol.* **24**, 208 (2005).
- C. N. Salinas, K. S. Anseth, *Biomaterials* **29**, 2370 (2008).
- A. M. DeLise, L. Fischer, R. S. Tuan, *Osteoarthritis Cartilage* **8**, 309 (2000).
- C. N. Salinas, B. B. Cole, A. M. Kasko, K. S. Anseth, *Tissue Eng.* **13**, 1025 (2007).
- The authors thank C. Bowman, T. Scott, and C. Kloxin for comments on early versions of this manuscript and valuable discussions; A. Aimetti for peptide synthesis training; J. McCall and S. Anderson for cell culture assistance; M. Schwartz for cell migration discussions; C. Bowman and his laboratory for use of and assistance with the rheometer and profilometer; C. Kloxin for assistance with image analysis; C. DeForest, Carl Zeiss, Inc., and the Howard Hughes Medical Institute Janelia Farms campus for assistance with and use of the Zeiss 710 two-photon confocal LSM; and the Howard Hughes Medical Institute and the NIH (grants DE12998 and DE16523) for research support. A.K. thanks the NASA Graduate Student Researchers Program fellowship and the Department of Education Graduate Assistance in Areas of National Need fellowship for support. A patent related to this work has been submitted (U.S. Patent Application No. 11/374,471).

Supporting Online Material

www.sciencemag.org/cgi/content/full/324/5923/59/DC1
Materials and Methods
SOM Text
Figs. S1 to S5
References

8 December 2008; accepted 3 February 2009
10.1126/science.1169494

Switchable Ferroelectric Diode and Photovoltaic Effect in BiFeO₃

T. Choi, S. Lee,* Y. J. Choi, V. Kiryukhin, S.-W. Cheong†

Unidirectional electric current flow, such as that found in a diode, is essential for modern electronics. It usually occurs at asymmetric interfaces such as p-n junctions or metal/semiconductor interfaces with Schottky barriers. We report on a diode effect associated with the direction of bulk electric polarization in BiFeO₃: a ferroelectric with a small optical gap edge of ~2.2 electron volts. We found that bulk electric conduction in ferroelectric monodomain BiFeO₃ crystals is highly nonlinear and unidirectional. This diode effect switches its direction when the electric polarization is flipped by an external voltage. A substantial visible-light photovoltaic effect is observed in BiFeO₃ diode structures. These results should improve understanding of charge conduction mechanisms in leaky ferroelectrics and advance the design of switchable devices combining ferroelectric, electronic, and optical functionalities.

Ferroelectrics undergo a transition from a high-symmetry structure to a low-symmetry state with a spontaneous electric polariza-

tion below a transition temperature. They usually consist of a complex microstructure of domains with different orientations of the polarization that

can be switched with external electric fields (1). Ferroelectrics are typically highly insulating because of large band gaps (2), and any current leakage has been considered to be a serious problem that deteriorates their functionalities (3, 4). The relationship between electronic transport characteristics and ferroelectric polarization has been little studied. This is partially due to complexity associated with ferroelectric domains. In addition, leakage often occurs through extended crystallographic defects such as grain boundaries or ferroelectric domain boundaries, so the true bulk leakage conduction may not be always dominant.

Rutgers Center for Emergent Materials and Department of Physics and Astronomy, Rutgers University, Piscataway, NJ 08854, USA.

*Present address: Neutron Science Division, Korea Atomic Energy Research Institute, Daejeon 305-353, Korea.

†To whom correspondence should be addressed. E-mail: sangc@physics.rutgers.edu